JB
Journals.ASM.org

# Multiple Roles of RNase Y in *Streptococcus pyogenes* mRNA Processing and Degradation

**Zhiyun Chen, Andreas Itzek, Horst Malke, Joseph J. Ferretti, Jens Kreth**

Department of Microbiology and Immunology, University of Oklahoma Health Sciences Center, Oklahoma City, Oklahoma, USA

**Control over mRNA stability is an essential part of gene regulation that involves both endo- and exoribonucleases. RNase Y is a recently identified endoribonuclease in Gram-positive bacteria, and an RNase Y ortholog has been identified in *Streptococcus pyogenes* (group A streptococcus [GAS]). In this study, we used microarray and Northern blot analyses to determine the *S. pyogenes* mRNA half-life of the transcriptome and to understand the role of RNase Y in global mRNA degradation and processing. We demonstrated that *S. pyogenes* has an unusually high mRNA turnover rate, with median and mean half-lives of 0.88 min and 1.26 min, respectively. A mutation of the RNase Y-encoding gene (*rny*) led to a 2-fold increase in overall mRNA stability. RNase Y was also found to play a significant role in the mRNA processing of virulence-associated genes as well as in the rapid degradation of *rnpB* read-through transcripts. From these results, we conclude that RNase Y is a pleiotropic regulator required for mRNA stability, mRNA processing, and removal of read-through transcripts in *S. pyogenes*.**

RNA degradation is a strictly regulated process that involves both endo- and exoribonucleases (1). In prokaryotes, mRNA degradation is initiated by endonucleolytic cleavage and followed by exonuclease digestion (2–4). The first step is relatively slow and rate limiting, while the second step proceeds rapidly (1). In *Escherichia coli*, RNase E functions as the major endoribonuclease that initiates the bulk of mRNA degradation (5). Although RNase E is absent in *Bacillus subtilis*, the recently identified RNase Y is considered its functional analog (6). RNase E and RNase Y do not share sequence homology but are strikingly similar in function (7, 8). Both RNases are membrane-bound proteins that interact with other components to form a complex called the RNA degradosome (7, 9). These components include other RNases, an RNA helicase, and two glycolytic enzymes (10, 11). Both RNase Y and RNase E prefer 5′ monophosphorylated RNA substrates with downstream secondary structures (6, 12). The depletion of *B. subtilis* RNase Y results in the accumulation of about 550 mRNAs, including important transcriptional regulators for stress response and biofilm formation and metabolic operons for tryptophan biosynthesis and glycolytic enzymes (8). *B. subtilis* RNase Y also interacts with RNases J1 and III to control the abundance of total mRNAs (13). RNase Y of *Staphylococcus aureus* plays a major role in virulence gene regulation and is involved in the processing and stabilization of a global regulator system, SaePQRS (14). These observations suggest that RNase Y is the major endoribonuclease in mRNA degradation in *B. subtilis* and perhaps also in other Gram-positive pathogens, such as *Streptococcus pyogenes*.

*S. pyogenes* (group A streptococcus [GAS]) causes a variety of human diseases ranging from mild local infections such as pharyngitis and impetigo to life-threatening systemic diseases such as toxic shock syndrome and necrotizing fasciitis (15). GAS infections often cause serious sequelae, including acute rheumatic fever, acute glomerulonephritis, and reactive arthritis (15). Transcriptional control of GAS virulence factor production has been investigated in detail, and several specific and global gene regulators have been identified (16–18). However, regulatory control of virulence factor production is more complex and includes the interplay of several regulatory circuits (19) and a multilayer control at the posttranscriptional level (20–23). For example, the mRNAs for streptolysin S (encoded by *sagA*) and streptodornase (encoded by *sda*) are greatly stabilized during entry into the stationary phase.

An RNase Y ortholog was recently identified in *S. pyogenes* (24). A mutation in the *S. pyogenes* RNase Y-encoding gene (*cvfA-rny*) altered the expression of multiple GAS virulence factors in a growth-dependent manner and attenuated the virulence of the GAS strain in a murine model (24). Unlike its counterpart in *B. subtilis*, *S. pyogenes* RNase Y is not an essential enzyme (24, 25). This property makes studies of the *S. pyogenes* RNase Y highly amenable to global analyses of its role in mRNA degradation and, ultimately, of the regulation of virulence.

Here we used microarray and Northern blot analyses to measure global *S. pyogenes* mRNA half-life and to determine the role of RNase Y in mRNA metabolism on the entire transcriptome. We demonstrate that *S. pyogenes* has an exceptionally high mRNA turnover rate and that RNase Y plays multiple roles in mRNA degradation, processing, and read-through transcript removal.

## MATERIALS AND METHODS

**Bacterial strains and growth conditions.** *S. pyogenes* NZ131 (M49) (26) and its *rny* gene mutant (Δ*rny*) (25) were routinely grown in C medium (0.5% proteose peptone no. 3; 1.5% yeast extract; 10 mM $K_2HPO_4$; 0.4 mM $MgSO_4$; 17 mM NaCl) (27) at 37°C without aeration. Erythromycin was added at a final concentration of 2 μg/ml when required. Bacterial growth curves were determined from three independent cultures with five technical replicates by using a BioScreen C machine (Piscataway, NJ).

**Total RNA extraction, cDNA synthesis, and microarray analysis.** Total RNA extraction, cDNA synthesis, and microarray analysis were car-

Received 22 January 2013 Accepted 22 March 2013

Published ahead of print 29 March 2013

Address correspondence to Jens Kreth, JKreth@ouhsc.edu, or Zhiyun Chen, Zhiyun-Chen@ouhsc.edu.

Supplemental material for this article may be found at http://dx.doi.org/10.1128/JB.00097-13.



doi:10.1128/JB.00097-13

ried out as described previously (25, 28), with slight modifications. Total RNA was extracted with TRIzol reagent (Invitrogen, Carlsbad, CA) and treated twice with Turbo DNase (Invitrogen) to remove chromosomal DNA. Fifteen micrograms of total RNA was used for cDNA synthesis with SuperScript II reverse transcriptase (Invitrogen). Two micrograms of cDNA was fragmented with DNase I (Roche, Indianapolis, IN) and 3′ end labeled with biotin-ddUTP using a BioArray terminal labeling kit (Enzo, New York, NY). A whole-genome custom GeneChip antisense expression microarray (16) was used for transcriptome analysis. On the antisense array, each gene of *S. pyogenes* was detected by a set of 17 25-mer oligonucleotide probes, and each intergenic region (IG) that was more than 100 bp in length was detected by a set of 25-mer probes, with gap widths ranging from 15 bp to 20 bp. ("Gap width" means the distance between the center nucleotides of two adjacent probes.) Hybridization, washing, and scanning of the custom *S. pyogenes* microarrays (16) were performed according to the procedures described by Affymetrix (Santa Clara, CA). Data sets were normalized based on stable RNA signals (rRNAs and tRNAs). Gene-level analysis was carried out by using the GeneChip operating software (GCOS) version 1.4 analysis program (Affymetrix). For probe-level analysis, the Affymetrix Power Tool (Affymetrx) was used to extract probe signal intensities from microarray CEL files.

**mRNA decay assay and Northern blot analysis.** mRNA decay is defined as the reduction in abundance of a transcript of defined size when no new transcript is synthesized. The mRNA decay assay and Northern blot analysis were carried out as mentioned previously, with slight modifications (25). Briefly, *S. pyogenes* cells were grown in C medium until the late exponential phase ($A_{600}$ = 0.50 to 0.55). Rifampin (1 mg/ml) and glucose (0.5% [wt/vol]) were added to the culture to inhibit new mRNA synthesis but maintain metabolic activity. Five-milliliter aliquots of the culture were withdrawn before ($t$ = 0 min) and after ($t$ = 0.5, 1, 2, 4, 8, 16, and 32 min) rifampin addition, rapidly chilled by mixing with 10 ml crushed ice, and harvested by centrifugation. For Northern blot analysis, total RNA was extracted with TRIzol reagent. One microgram of total RNA was separated on a denaturing agarose gel, transferred to a Hybond-N membrane (Amersham), and immobilized to the membrane by UV cross-linking (Stratalinker 1800 crosslinker; Stratagene). RNA probes were generated by T7 *in vitro* transcription (New England BioLabs, Ipswich, MA) of PCR fragments amplified with the primers listed in Table 1. Digoxigenin (DIG) was incorporated into RNA probes by replacing 25% standard UTP with DIG-UTP (Roche) in the *in vitro* transcription reaction. DIG-labeled RNA probes were hybridized to membrane-bound RNA targets at 68°C overnight. Signal visualization was achieved by using anti-DIG antibody and CDP-*Star* according to the manufacturer's instructions (DIG application manual; Roche Diagnostic). The abundance of gene transcripts, represented by the average pixel intensity of defined band sizes, was quantified with ImageJ software version 1.44o (29). 16S rRNA was visualized by ethidium bromide staining on an agarose gel prior to transfer and served as loading control.

**mRNA half-life calculation.** We developed a "steepest-slope" method to calculate *S. pyogenes* mRNA half-life. A typical mRNA decay process included a delay phase, a decay phase, and/or a stabilized phase (see Fig. S1 in the supplemental material). The most rapid mRNA reduction occurred in the decay phase, which constituted the steepest downward slope when plotted against decay time (see Fig. S1 in the supplemental material). The aim of this method was to identify the time range in which the most rapid mRNA reduction occurred. Two variables, $t_i$ and $t_j$, were used to define the starting ($t_i$ = 0, 0.5, 1, 2, 4, or 8 min after rifampin addition) and ending ($t_j$ = 1, 2, 4, 8, 16, or 32 min after rifampin addition) points of a particular time range during an mRNA decay assay. At least one time point was included between $t_i$ and $t_j$ so that the half-life estimation was based on at least three consecutive time points. Exponential regression was carried out to determine the slope of the mRNA decay curve in each given time range defined by $t_i$ and $t_j$, assuming that mRNA decay followed first-order kinetics, as demonstrated before (30). The time range that displayed the steepest downward slope of mRNA decay was considered the decay phase, and the mRNA half-life was calculated accordingly. Poorly expressed genes with microarray signals of less than 200 throughout the mRNA decay assay usually did not display an obvious mRNA decay phase and were excluded from half-life calculations.

**TABLE 1** Primers used in this study

| Primer | Sequence[a] |
|---|---|
| upp_1L | CGTCGTCAAACCACATCAAC |
| upp_1R(T7) | TAATACGACTCACTATAGGGCCCAAATAAACGATCACCA |
| pepC_1L | AACCCGTCAAAGTGAAGTGG |
| pepC_1R(T7) | TAATACGACTCACTATAGGGAAACCAAACGGACTCACCAG |
| ptsI_1L | CATGAATGGCAAACCTGTTG |
| ptsI_1R(T7) | TAATACGACTCACTATAGGGTTCTGTAAGCGCACGATTTG |
| cfa_1L | TGATGCTTCAAATCCCGATA |
| cfa_1R(T7) | TAATACGACTCACTATAGGGGGTTTGATCCCCAAAACCTT |
| ska_1L | GTTGAGGGGACGAATCAAGA |
| ska_1R(T7) | TAATACGACTCACTATAGGGATTGGGCAATTGCTGCTAAC |
| ropB_1L | GGAAATTGGTGAAACCGTTG |
| ropB_1R(T7) | TAATACGACTCACTATAGGGAAACATATGATGGATCGTTTTGC |
| recA_1L | TGATCCAGCTTATGCTGCTG |
| recA_1R(T7) | TAATACGACTCACTATAGGACAAGCTCCCCTGTACGAGA |
| sodM_1L | GTTTGATGCGGAGACAATGA |
| sodM_1R(T7) | TAATACGACTCACTATAGGGGCGGCTTGGTAAAGTTCTGA |
| emm49_1L | CGTGTCTAGCGTTGCAAGAA |
| emm49_1R(T7) | TAATACGACTCACTATAGGGTCAAGGGCTTGAAGTTTGC |
| tufA_1L | CCAGGTGATGACCTTCCAGT |
| tufA_1R(T7) | TAATACGACTCACTATAGGGACCTTGTTCTACGGCGATTG |
| rnpB_F | GCAATTTTTGGATAATCGCGTA |
| rnpB_R(T7) | TAATACGACTCACTATAGGGTTTTGTTCCGGAAATAACTAGGA |
| Spy49_1274_F | TGGTGAAGCTGTACGCAAAC |
| Spy49_1274_R(T7) | TAATACGACTCACTATAGGGTTTGCTCTTTGTGGCATCTG |
| Spy49_1275_F | TCAGGCGATTACCAAAAAGG |
| Spy49_1275_R(T7) | TAATACGACTCACTATAGGGCTTGCAGACGCATTTGCTTA |
| Spy49_1276_1L | TGCGAGGGTTTGATAAGAAAG |
| Spy49_1276_1R(T7) | TAATACGACTCACTATAGGGCCAAAAACCTCTTTTTCCAATTT |
| fasX_F | CGAAGTCATGAGTTTATCGAGCA |
| fasX_R(T7) | TAATACGACTCACTATAGGGTGATATCCAAACAAAGACAACTGA |
| Anchor | TTTAGTGAGGGTTAATAAGCGGCCGCGTCGTGACTGGGAGCGC |
| T3 | GCGGCCGCTTATTAACCCTCACTAAA |
| ropB_R(RACE) | TGACCAAGGCAAAAAGGTTC |

[a] T7 promoter sequences are underlined.

**5′ RACE.** To determine the transcriptional start sites (TSS) of genes, 5′ rapid amplification of cDNA ends (5′ RACE) was carried out by following the protocol described by Troutt et al. (31), with modification. Briefly, 200 ng *S. pyogenes* wild-type (WT) cDNA was ligated to 10 nmol 5′ phosphorylated anchor primer with T4 RNA ligase (Ambion) in a 20 μl reaction mixture. Dimethyl sulfoxide (DMSO) was added to the mixture to reach a final concentration of 10% (vol/vol) to relax secondary structures. The reaction mixture was incubated at 23°C for 18 h, heated at 65°C for 15 min to inactivate T4 RNA ligase, and subsequently used as the PCR template. PCR was carried out by using a forward primer (T3) complementary to the anchor primer and a reverse primer specific to the target gene, and the PCR product was subsequently sequenced to determine the TSS.

**Statistical analyses.** One-way analysis of variance (ANOVA) and histogram analyses were carried out by using the Statplus statistical program (Analystsoft).

**Microarray data accession number.** The microarray data sets were deposited in the Gene Expression Omnibus (GEO) database under platform GPL11420 with accession number GSE40198.

## RESULTS

**Transcriptome profiles of the WT and isogenic Δ*rny* mutant strains.** The isogenic NZ131 Δ*rny* mutant strain was constructed as described previously (25). The deletion of the *S. pyogenes rny* gene caused a slight slowdown of bacterial growth, with the generation time increasing from 50 min to 57 min (Fig. 1A). Microarray analysis of the WT and Δ*rny* mutant strains in the late exponential phase ($A_{600}$ = 0.5 to 0.55) showed very similar transcriptome profiles (Fig. 1B). Among 1,704 examined open

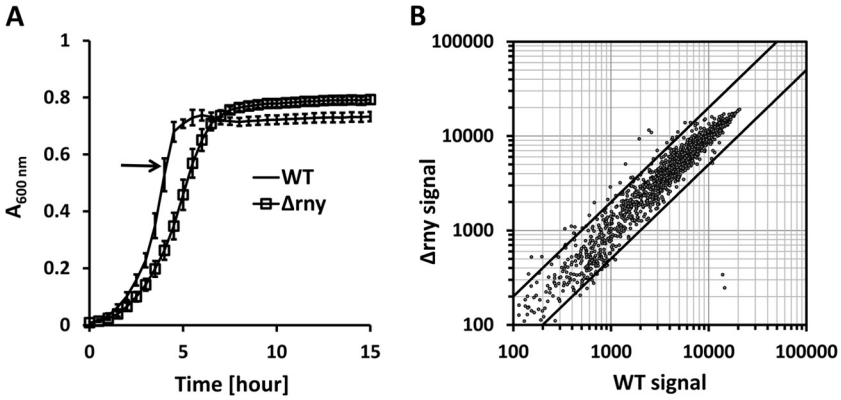


**FIG 1** Transcriptome analysis of the WT and RNase Y mutant (Δ*rny*). (A) Growth curves of the WT and the Δ*rny* mutant in C medium (means ± standard deviations [SD]; $n = 5$). Samples were collected in the late exponential phase (optical density at 600 nm [$OD_{600}$] = 0.50 to 0.55) for transcriptome analysis. (B) Microarray signals of the Δ*rny* mutant were plotted against signals of the WT on a log-scale scatter diagram. The two diagonal lines indicate a 2-fold difference in microarray signal values between the two strains. Averages of the results of three biological replicates are presented.

reading frames (ORFs), 97.8% displayed a less than 2-fold difference between the two strains in transcript abundance. Only the expression of *speB* (streptococcal pyrogenic exotoxin B) and *spi* (SpeB inhibitor) was significantly reduced in the Δ*rny* mutant, which is consistent with previous observations (24, 25). About 30 genes were significantly increased in expression in the Δ*rny* mutant, including *speG* (exotoxin type G precursor), *ypaA* (riboflavin transporter), and two genes encoding hypothetical proteins (Spy49_1275 and Spy49_1276). Subsequent analyses showed that the mRNAs of these genes were greatly stabilized in the Δ*rny* mutant (Table 2) (see below).

**mRNA half-life calculation.** In order to examine global mRNA half-life, a steepest-slope method was developed based upon microarray data sets (see Materials and Methods for details) and was compared to two established methods proposed by Steglich et al. (32) and Selinger et al. (30). Specifically, Steglich's method defined the mRNA decay phase as the time range in which the exponential regression of decay displayed the minimal mean square error (32). Selinger's method defined the mRNA decay phase as the time range starting from $t = 0$ min to the earliest time point that displayed a decrease in mRNA abundance of more than 2-fold (30). We used the three methods to calculate *S. pyogenes* WT mRNA half-life and obtained consistent results ($R^2 = 0.78$ between the steepest-slope and Steglich's methods and 0.89 between the steepest-slope and Selinger's methods) (see Fig. S2 in the supplemental material). Nevertheless, major differences were observed in highly abundant mRNAs, for which the steepest-slope method yielded smaller half-life estimations than the other two methods.

In order to evaluate the accuracy of the three methods, Northern blot analysis was carried out to determine the actual half-lives of 12 highly expressed mRNAs with a broad range of half-lives. Results showed that the steepest-slope method yielded mRNA

**TABLE 2** Microarray analysis of selected genes described in this study

| Locus | Gene | Abundance (microarray signal)[a] | | | Half-life (min) (microarray based) | | | Function |
|---|---|---|---|---|---|---|---|---|
| | | WT | Δ*rny* mutant | Ratio | WT | Δ*rny* mutant | Ratio | |
| Spy49_0187 | *speG* | 1,946 | 9,342 | 4.8 | 0.31 | 7.44 | 23.8 | Exotoxin type G precursor |
| Spy49_0307 | *ypaA* | 2,442 | 11,543 | 4.7 | 0.31 | 12.79 | 41.9 | Riboflavin transporter |
| Spy49_0322 | *upp* | 10,747 | 8,564 | 0.8 | 1.10 | 1.39 | 1.3 | Uracil phosphoribosyltransferase |
| Spy49_0515 | *tufA* | 13,502 | 13,638 | 1.0 | 7.63 | 21.13 | 2.8 | Translation elongation factor Tu |
| Spy49_1010 | *cfa* | 10,909 | 9,374 | 0.9 | 6.89 | 6.73 | 1.0 | CAMP factor |
| Spy49_1094 | *ptsI* | 14,665 | 13,475 | 0.9 | 2.83 | 3.49 | 1.2 | Phosphoenolpyruvate-protein phosphotransferase of phosphotransferase system |
| Spy49_1122 | *sodM* | 14,655 | 14,282 | 1.0 | 7.06 | 8.57 | 1.2 | Superoxide dismutase (Mn) |
| Spy49_1274 | | 6,740 | 11,315 | 1.7 | 0.85 | 9.17 | 10.8 | Hypothetical protein |
| Spy49_ig0545 | *rnpB* | 15,954 | 15,035 | 0.9 | 40.33 | 34.74 | 0.9 | RNA subunit of RNase P |
| Spy49_1275 | | 5,719 | 13,845 | 2.4 | 0.52 | 12.93 | 24.7 | Hypothetical protein |
| Spy49_1276 | | 6,508 | 13,878 | 2.1 | 0.25 | 13.09 | 53.0 | Conserved hypothetical protein |
| Spy49_1280 | *pepC* | 9,698 | 10,397 | 1.1 | 1.48 | 3.47 | 2.3 | Aminopeptidase C |
| Spy49_1630 | *ska* | 10,995 | 9,202 | 0.8 | 4.52 | 3.75 | 0.8 | Streptokinase |
| Spy49_1671 | *emm49* | 11175 | 11,731 | 1.0 | 2.57 | 4.94 | 1.9 | Antiphagocytic M protein |
| Spy49_1689 | *spi* | 14,553 | 247 | 0.0 | 8.04 | 5.59 | 0.7 | SpeB protease inhibitor |
| Spy49_1690 | *speB* | 13,889 | 340 | 0.0 | 8.71 | 6.18 | 0.7 | Streptococcal pyrogenic exotoxin B |
| Spy49_1691 | *ropB* | 5,813 | 4,807 | 0.8 | 0.87 | 0.85 | 1.0 | Rgg-like transcription regulator |
| Spy49_1753 | *recA* | 9,878 | 11,096 | 1.1 | 0.87 | 2.92 | 3.4 | RecA protein |

[a] Abundance data represent average band intensities in pixels.

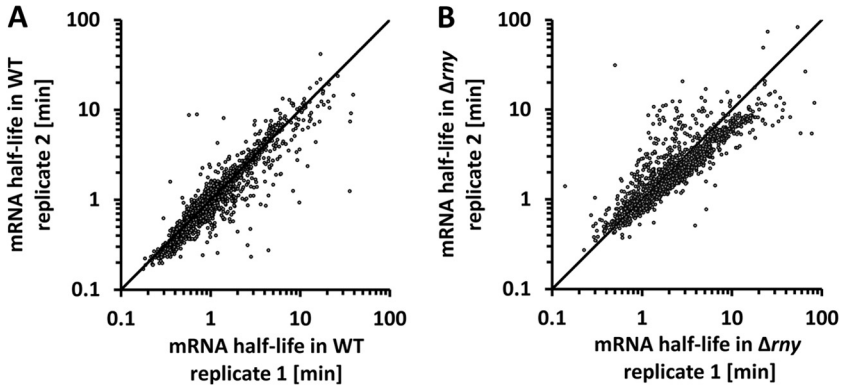


**FIG 2** Consistency of mRNA half-life estimations between biological replicates. mRNA half-lives obtained from two biological replicates of the WT (A) and Δ*rny* mutant (B) were plotted against each other on a log-scale scatter diagram. The diagonal line is used for visual determination of data consistency.

half-lives that were closest to the actual values, while the other two methods overestimated them (see Fig. S3 in the supplemental material). These highly expressed mRNAs caused signal saturation on microarray chips, especially at the beginning of a decay assay. Selinger's and Steglich's methods were susceptible to the signal saturation and would overestimate the half-life, though the steepest-slope method was much more tolerant of signal saturation and would give a correct estimation as long as there was an obvious decay phase. An exception was observed in *sodM* (superoxide dismutase), the half-life of which was determined to be 0.69 min by Northern blotting (see Fig. 5 below) and was overestimated by all three microarray-based methods (7.06 min, 18.2 min, and 12.04 min by the steepest-slope, Steglich's, and Selinger's methods, respectively). Closer examination revealed that *sodM*-specific probe signals were saturated throughout the decay assay except for the last time point, which suggested that the *sodM* mRNA level was far beyond the dynamic range of the microarray. In such a case, optimizing the calculation method itself could not solve the bias problem. Thus, for our assay conditions, the steepest-slope method was the most reliable approach to estimate global mRNA half-life.

**mRNA stability profiles in the WT and Δ*rny* strains.** Microarray analysis and the steepest-slope method were used to estimate mRNA half-lives in the genomes of the WT and the Δ*rny* mutant. Measurements were performed using two independent biological replicates. Results from the replicates showed high consistency for both strains (Fig. 2), which confirmed the reliability of our measurements and half-life calculation. Averaged mRNA half-lives were further used for analyses. Poorly expressed genes were excluded because of their indeterminate mRNA decay phases. Prophage genes were also excluded because of their significant heterogeneity from nonprophage genes. Specifically, the prophage mRNA abundance was 4-fold lower than that of nonprophage mRNAs, while the mean half-life was five times higher than that of the latter (7.5 min versus 1.24 min). In the end, we obtained the mRNA half-lives of 1,485 genes (87.1% of the whole genome) (see Dataset S1 in the supplemental material).

The median and mean half-lives of *S. pyogenes* mRNAs in the WT, when estimated with the steepest-slope method, were 0.89 min and 1.24 min, respectively. In the Δ*rny* mutant, these values increased to 1.81 min and 2.79 min. In the WT, 1,267 genes had an mRNA half-life of less than 2 min (unstable mRNAs) and only 34 genes had an mRNA half-life of longer than 5 min (stable mRNAs) (Fig. 3A). In the Δ*rny* mutant, the number of unstable mRNAs was reduced to 826 and the number of stable mRNAs increased to 178 (Fig. 3A). The effects of the *rny* mutation appeared to be similar

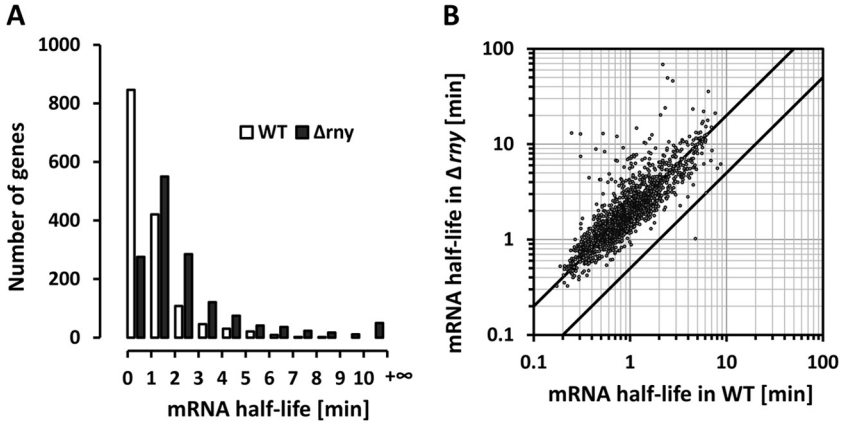


**FIG 3** Effects of RNase Y mutation on mRNA stability. (A) Distribution of mRNA half-lives in the WT and Δ*rny* mutant. Half-life rates averaged from two biological replicates were categorized in 1-min increments. (B) Correlation of mRNA half-lives in the WT and the Δ*rny* mutant. The two diagonal lines indicate a 2-fold difference in mRNA half-life between the two strains.

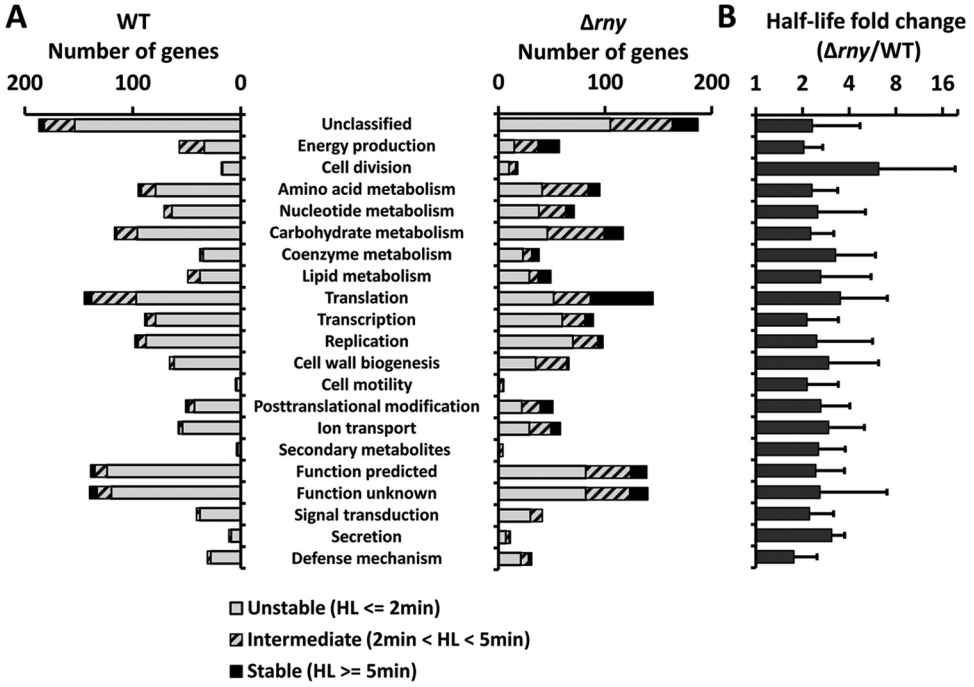


**FIG 4** mRNA half-life (HL) in different functional groups. *S. pyogenes* genes were grouped based on COGs. (A) The numbers of unstable, intermediate, and stable mRNAs in the WT and Δ*rny* mutant were counted for each functional group. (B) The fold changes of mRNA half-life caused by the *rny* gene mutation were calculated for each functional group.

for the majority of *S. pyogenes* mRNAs, with a 2-fold increase in overall mRNA stability (Fig. 3B). One-way ANOVA showed that the differences between the two strains in mRNA stability were statistically significant ($P < 0.001$).

We also used Selinger's and Steglich's methods to estimate overall *S. pyogenes* mRNA half-lives in the two strains. Selinger's method showed 1.02 min and 1.65 min for median and mean mRNA half-lives in the WT and 2.39 min and 3.62 min in the Δ*rny* mutant. Steglich's method showed 1.20 min and 1.84 min for median and mean mRNA half-lives in the WT and 2.35 min and 4.18 min in the Δ*rny* mutant. Both results showed an approximately 2-fold increase in mRNA stability in the Δ*rny* mutant, which was in agreement with our observation using the steepest-slope method.

**mRNA stability and gene function.** We hypothesized that genes belonging to different functional groups might have different mRNA stabilities. To test this hypothesis, *S. pyogenes* genes were categorized based on COGs (Clusters of Orthologous Groups) (33), and their mRNA half-lives in the WT were compared between functional groups (Fig. 4). One-way ANOVA indicated that significant differences in mRNA half-life existed in various functional groups ($P < 0.001$). Specifically, mRNAs involved in energy production and translation had a longer half-life than average ($P < 0.001$). For example, genes encoding ATP synthase (Spy49_0582 to Spy49_0589) and genes encoding ribosomal proteins (57 genes in total) had average mRNA half-lives of 3.9 min and 3.0 min in the WT, respectively, and those half-lives were significantly longer than the overall mRNA half-life (1.24 min). In contrast, all mRNAs involved in cell division and signal transduction were unstable mRNAs (half-life < 2 min), with average half-lives of 0.89 min and 1.01 min, respectively. However, the difference between these two groups and the whole genome was not statistically significant ($P > 0.05$). The vast majority of mRNA half-lives increased in the Δ*rny* mutant, though the stability profiles among the functional groups remained similar to what was observed in the WT. These observations support our hypothesis that mRNA stability is related to the function of the gene product and are in agreement with previous findings in other species (34, 35).

Previous studies suggested the possibility that *E. coli* RNase E, the functional analog of RNase Y, might preferentially cleave mRNAs in certain functional groups (36). To determine whether RNase Y has a similar preferentiality in GAS, we compared the changes in mRNA half-life between the WT and Δ*rny* mutant in each functional group (Fig. 4). In general, the *rny* gene mutation resulted in a 1.7- to 3.3-fold increase in mRNA half-life in all groups except for the cell division group that displayed a 6.2-fold increase in mRNA half-life. Closer examination shows that this group contained a gene locus (Spy49_1276) that was stabilized more than 30-fold in the Δ*rny* mutant (see below for details). All other genes in this group were stabilized 2- to 3-fold, which is similar to levels seen with the other functional groups. One-way ANOVA indicated that the difference between functional groups with respect to half-life fold changes caused by the *rny* gene mutation was not significant ($P > 0.05$). Therefore, we found no evidence suggesting that RNase Y preferentially degraded mRNAs from certain functional groups.

**Differential effects of RNase Y on mRNA stabilities.** While our results revealed a 2-fold increase in overall mRNA stability in the *rny* background (Fig. 3B), some mRNAs were unaffected or even slightly destabilized and others were greatly stabilized (Table 2). To confirm these findings, we selected a set of RNAs

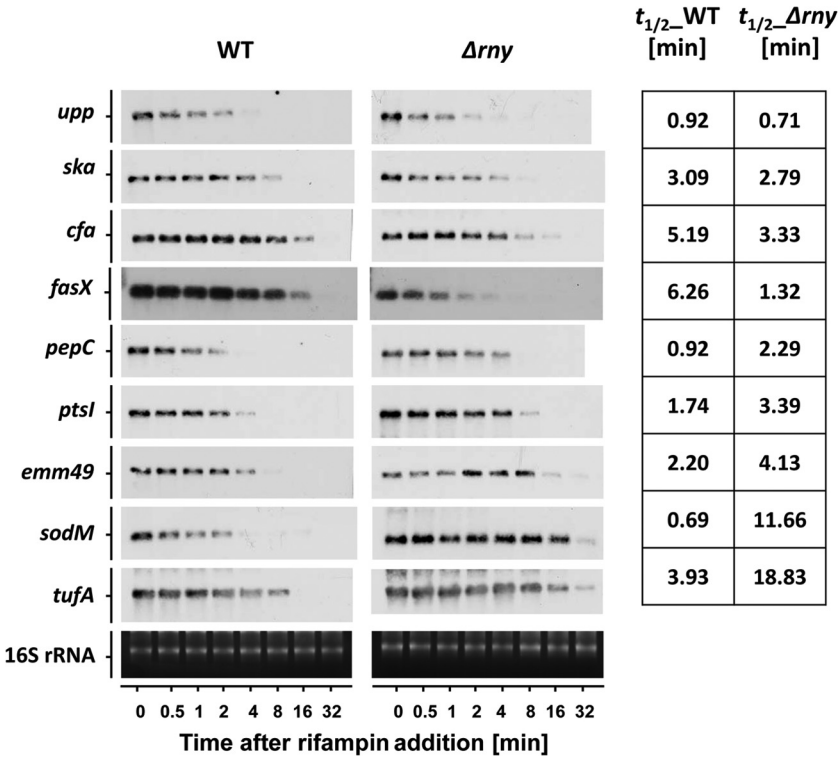


| $t_{1/2}$_WT [min] | $t_{1/2}$_Δrny [min] |
|---|---|
| 0.92 | 0.71 |
| 3.09 | 2.79 |
| 5.19 | 3.33 |
| 6.26 | 1.32 |
| 0.92 | 2.29 |
| 1.74 | 3.39 |
| 2.20 | 4.13 |
| 0.69 | 11.66 |
| 3.93 | 18.83 |

**FIG 5** Northern blot analysis of mRNAs that were differentially affected by *rny* gene mutation. The respective Northern blots are shown for the wild type and the Δ*rny* mutant for the listed genes. The blots demonstrate the decay of mRNA transcripts after rifampin addition. Each blot experiment was carried out twice. The averaged half-lives in minutes are presented in the right column for the wild type and the Δ*rny* mutant.

displaying differential stabilities and examined their half-lives with Northern blot analysis. The results showed no significant change in *upp*, *ska*, and *cfa* mRNA stabilities, a 2- to 3-fold increase in *pepC*, *ptsI*, and *emm49* stabilities, and a 5-fold or greater increase in *sodM* and *tufA* stabilities (Fig. 5). We also examined the stability of *fasX*, which is a small noncoding RNA that stabilizes *ska* mRNA (21). Surprisingly, the *fasX* RNA was very stable in the WT (half-life $>$ 6 min) but was considerably destabilized in the Δ*rny* mutant (half-life $<$ 2 min). Meanwhile, the abundance of *fasX* RNA in the WT was more than 2-fold higher than in the Δ*rny* mutant (Fig. 5A and data not shown). The decreased *fasX* transcript abundance in the Δ*rny* may directly result from the high RNA degradation rate, though other regulatory mechanisms may also be involved. The whole *S. pyogenes* transcriptome, including ORFs and intergenic regions, was screened for destabilized RNAs in the Δ*rny* mutant, and only *fasX* has been identified so far (data not shown). These findings suggest that RNase Y plays different roles in degrading different RNA targets.

**RNase Y functions in mRNA processing.** Northern blot analysis revealed that RNase Y is involved in the processing of *ropB* (*rgg*) mRNA (Fig. 6A). The *ropB* gene encodes a transcriptional regulator that activates the streptococcus exotoxin B-encoding gene (*speB*) (27, 37). The two genes locate next to each other on the chromosome in opposite orientations (38). Northern blot analysis showed that, in the WT, the *ropB* locus specifies three transcripts of different sizes (1.2 kb, 1.1 kb, and 1.0 kb, respectively) (Fig. 6A). The 1.2-kb *ropB* transcript was less abundant and degraded faster than the two shorter transcripts. In the Δ*rny* mutant, the 1.2-kb transcript became the most prominent form of *ropB* mRNA, while the 1.0-kb transcript was less abundant and the 1.1-kb transcript was undetectable (Fig. 6A). The 1.2-kb transcript was stabilized only slightly in the Δ*rny* mutant, which suggested that its increased abundance was not due to increased stability (Fig. 6A). Rather, our results suggest that the 1.2-kb transcript could be the primary *ropB* transcript that underwent endonucleolytic cleavages to generate the 1.1-kb and 1.0-kb transcripts. These results also suggested that RNase Y was very likely the enzyme responsible for *ropB* mRNA processing.

We next used 5′ RACE to determine the 5′ ends of three *ropB* mRNA transcripts. The *ropB* transcripts were expected to have identical 3′ ends but different 5′ ends, since the *ropB* gene had a strong Rho-independent terminator immediately downstream of the coding region (data not shown). The 5′ end of the 1.0-kb *ropB* transcript was determined to be 139 nucleotides (nt) upstream of the *ropB* translational start site. We were unable to determine the 5′ ends of the other two transcripts, presumably because of the complicated secondary structures in that region. Based on transcript sizes, the 5′ ends of the 1.2-kb and 1.1-kb transcripts were predicted to be 300 to 400 nt and 200 to 300 nt upstream of the translational start site, respectively (Fig. 6B). The *speB* gene TSS had been previously determined to be 244 bp upstream of the *ropB* translational start site (38), which was confirmed in this study (Fig. 6B). These findings suggested that the *ropB* and *speB* promoters overlapped in opposite directions on the chromosome.

The *ropB* mRNA was further analyzed using our microarray data. Probe-level analysis showed an abrupt upshift of probe signal intensity at approximately 350 nt upstream of the *ropB* translational start site (Fig. 6B), which strongly suggests that the *ropB*

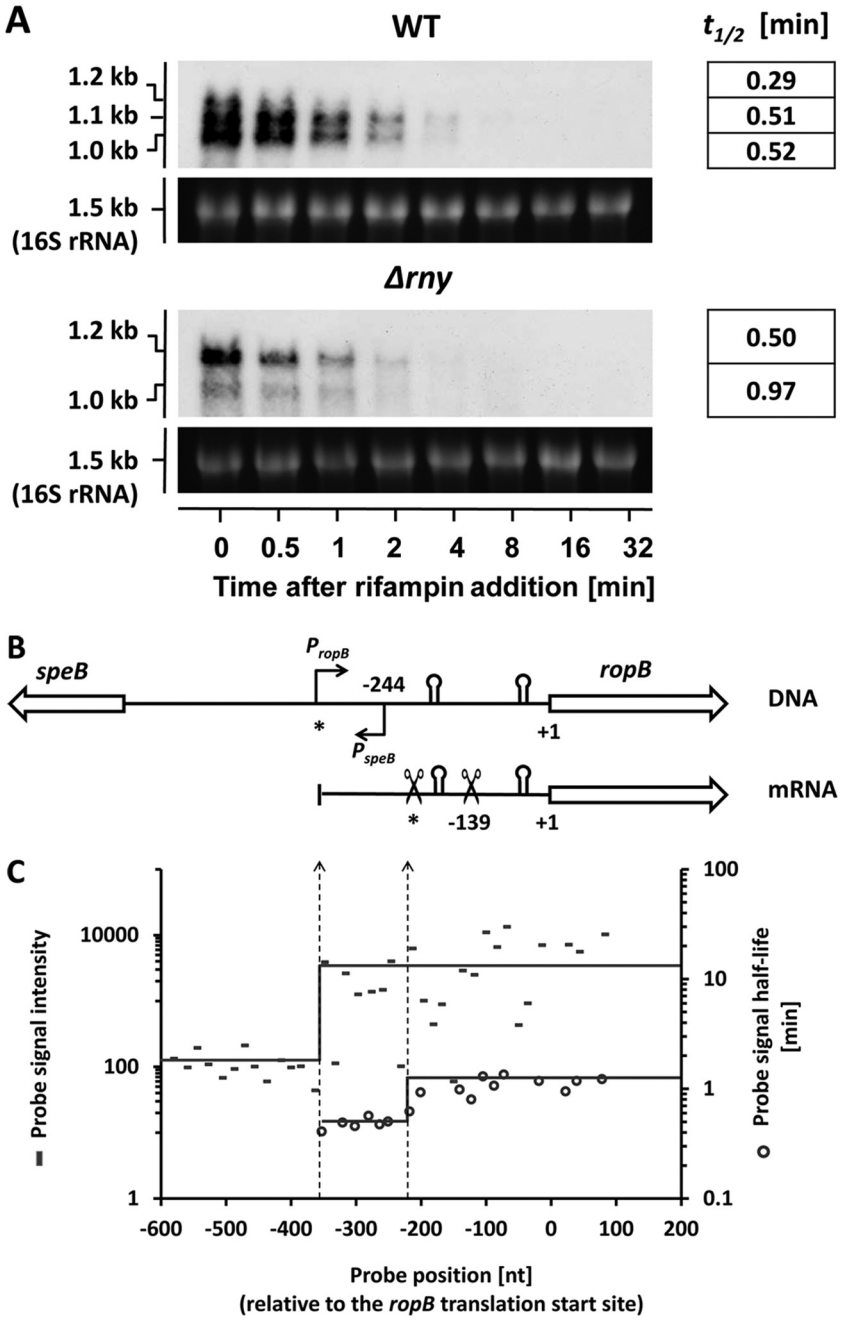


**FIG 6** Northern blot and probe-level analyses of the *ropB* mRNA. (A) Estimation of the *ropB* transcript half-lives in the WT and the Δ*rny* mutant with Northern blot analysis. Each blot experiment was carried out twice. The averaged half-lives (in minutes) are presented in the right column. (B) Arrangements of the *ropB* and *speB* genes on the chromosome and the *ropB* mRNA structure. The *ropB* and *speB* promoters are indicated as bent arrows. Two pairs of inverted repeats in the *ropB* 5′ UTR are indicated as stem-loop structures. Two putative cleavage sites are indicated with scissor symbols. The predicted *ropB* TTS and the first putative cleavage site are marked with asterisks. (C) Probe-level analysis of the *ropB* mRNA. The average probe signal intensities upstream and downstream of the predicted *ropB* TTS are shown as solid lines (dashes indicate individual results). The average probe signal half-lives upstream and downstream of the first putative cleavage site are also shown as solid lines (open circles indicate individual results). The left and right dotted vertical lines indicate the shifts of the probe signal intensities and probe signal half-life, which correspond to the *ropB* TTS and the first putative cleavage site, respectively.

TSS was in that region. It also showed an upshift of probe signal half-life at approximately 210 nt upstream of the *ropB* translational start site, with average probe half-life increasing from 0.50 min to 1.16 min (Fig. 6B). The upshift was likely due to the differential stabilities of primary (1.2-kb) and processed (1.1-kb and 1.0-kb) *ropB* transcripts (Fig. 6B).

**RNase Y degrades *rnpB* read-through transcripts.** Microarray analysis showed that the *rny* mutation significantly stabilized the mRNAs of three consecutive hypothetical gene open reading frames, Spy49_1274, Spy49_1275, and Spy49_1276 (Table 2). A BLASTP search indicated that Spy49_1274 encodes a Holiday junction-specific endonuclease, Spy49_1275 encodes a putative

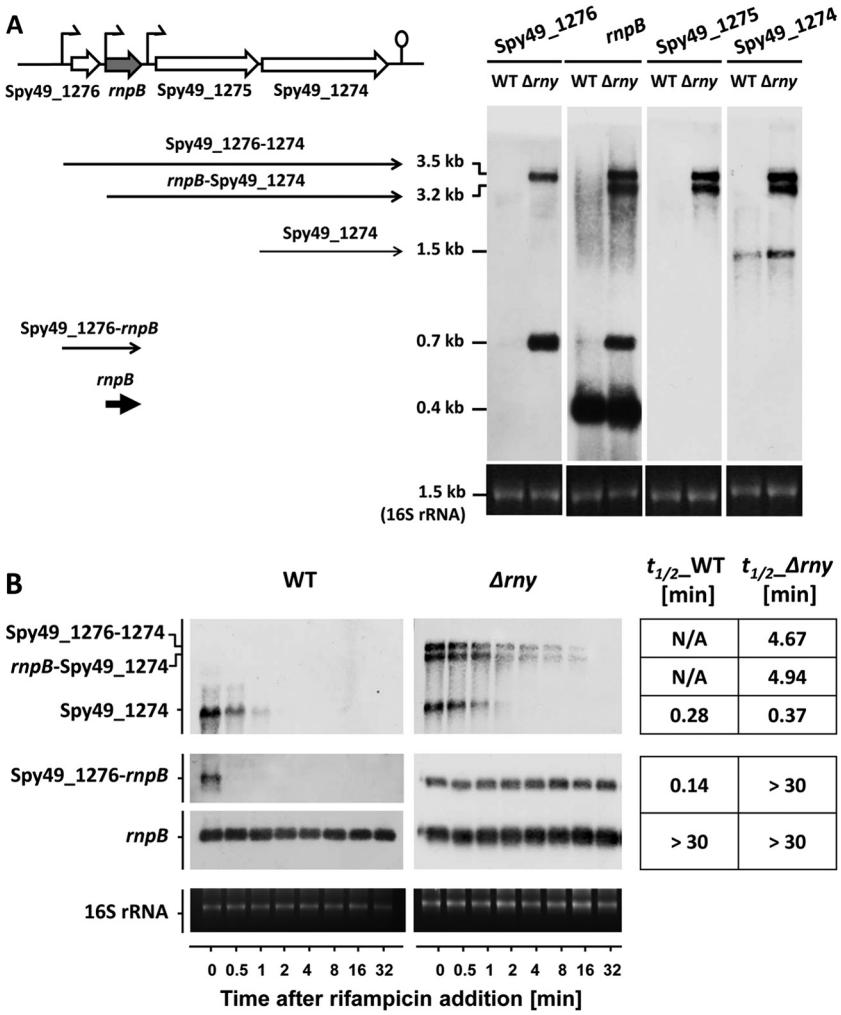


**FIG 7** The Spy49_1274-Spy49_1276 region. (A) Chromosomal arrangement of the Spy49_1274-Spy49_1276 region and Northern blot analysis of their transcripts. (B) The mRNA stabilities of Spy49_1274 and *rnpB* read-through transcripts were determined by Northern blotting. Each blot experiment was carried out twice. The averaged half-lives (in minutes) are presented in the right column.

RNA methyltransferase, and Spy49_1276 encodes a cell division initiation protein that is highly homologous to the GpsB protein in *B. subtilis* (39). The Spy49_1274 and Spy49_1275 genes are organized as a bicistronic operon, while Spy49_1276 is located 491 bp upstream of the operon (Fig. 7A). Sequence analysis showed that the intergenic region between Spy49_1276 and the Spy49_1275-Spy49_1274 operon contained an *rnpB* gene encoding the RNA component of RNase P. RNase P is an essential ribozyme that catalyzes the 5′ processing of pre-tRNAs (40).

The *rnpB* transcript itself was extremely stable (with a half-life of longer than 30 min) and highly abundant in *S. pyogenes*, though the transcripts of its surrounding genes (Spy49_1274, Spy49_1275, and Spy49_1276) were less abundant and very unstable in the WT, with an mRNA half-life of less than 1 min (Table 2). Their mRNA stabilities were greatly enhanced in the Δ*rny* mutant, with half-life increasing to longer than 10 min, making them the mRNAs most profoundly affected by RNase Y in the *S. pyogenes* genome. The steady-state levels of these mRNAs also increased dramatically in the Δ*rny* mutant compared to the WT (Table 2). Our subsequent Northern blot analyses showed that it was the accumulation of *rnpB* read-through transcripts, rather than the stabilization of primary transcripts, that caused the increased expression of the genes surrounding *rnpB*. The *rnpB* upstream gene (Spy49_1276) did not have a strong terminator at its 3′ end and was cotranscribed with *rnpB* to form a 0.7-kb transcript (Fig. 7A). This transcript was poorly expressed and very unstable in the WT but became highly abundant and extremely stable in the Δ*rny* mutant (Fig. 7). We were unable to detect the full-length Spy49_1275-Spy49_1274 transcript and could detect only the Spy49_1274 single-gene transcript (Fig. 7A). It was possible that the full-length Spy49_1275-Spy49_1274 transcript underwent processing to generate two single-gene transcripts and that the Spy49_1274 transcript was more stable than the Spy49_1275 transcript. The *rny* mutation stabilized the Spy49_1274 single-gene mRNA only slightly, with the half-life increasing from 0.28 min to 0.56 min (Fig. 7B). Meanwhile, two long read-through transcripts that were transcribed from the Spy49_1276 and *rnpB* promoters emerged in the Δ*rny* mutant. The read-through transcripts were not detectable in the WT but were highly abundant and very stable in the Δ*rny* mutant (Fig. 7A). These observations suggested that

RNase Y was involved in the rapid degradation of *rnpB* read-through transcripts.

## DISCUSSION

In this study, we examined *S. pyogenes* mRNA stability and the role of RNase Y in mRNA degradation on a transcriptome-wide scale. To the best of our knowledge, this is the first attempt to determine precisely the global mRNA half-life in an obligate human pathogen. Our results showed that *S. pyogenes* had a higher mRNA turnover rate than other bacteria with known global half-lives. With our newly developed steepest-slope method, the median half-life of *S. pyogenes* mRNAs was estimated to be 0.89 min, with about 85% of mRNA half-lives being less than 2 min. Similar short mRNA half-life estimations were made by using two established half-life calculation methods (see Results), which suggested that the observed high *S. pyogenes* mRNA turnover rate was not a method bias. In contrast, the median half-life of *Bacillus cereus* mRNAs was estimated by different groups to be 2.4 min (35) and 5 min (41). In *E. coli*, about 80% of mRNAs had a half-life of between 3 and 8 min (34). In *Staphylococcus aureus*, about 90% of mRNAs had a half-life of less than 5 min, though the exact values were not determined (14).

The *rny* gene mutation led to a 2-fold increase in overall mRNA half-life without significantly affecting the steady-state levels of most mRNA species. Similar observations were made by Kang et al., who reported that the differential gene transcription caused by an *rny* mutation was not obvious in the exponential phase (24). These observations seem to contradict each other, since one would expect that increased mRNA stability would cause increased mRNA abundance. However, this expectation is based on the assumption that the mRNA synthesis rate remains unaltered in the Δ*rny* mutant, which may not be the case. We believe that these seemingly contradicting observations may be explained by the following observations. (i) Gene transcription, but not mRNA degradation, is the dominant factor that determines the mRNA steady-state level. This notion was suggested by Bernstein et al., as they observed increased global mRNA stability but unaltered mRNA abundance in the *E. coli* RNase E mutant (34). (ii) Decreased mRNA turnover rate may reduce the free nucleotide pool, which in turn may slow down new mRNA synthesis. (iii) The organism may use other strategies to detect mRNA abundance and adjust mRNA synthesis accordingly. The rapid mRNA turnover rate of *S. pyogenes* may have alternative roles, perhaps including facilitation of adaptation of the organism to fast-changing environments at different stages of bacterial infection. It would be intriguing to understand whether the rapid mRNA turnover is a unique feature of *S. pyogenes* or a common theme in other streptococci and/or in other human pathogens when such data sets become available.

*fasX*, a small regulatory RNA, was severely destabilized in the Δ*rny* mutant. This small RNA enhances streptokinase activity by base pairing to the 5′ end of *ska* mRNA and stabilizing the transcript (21). However, the *ska* mRNA stability did not change significantly in the Δ*rny* mutant (this study and reference 21). This finding may be attributable to the stabilizing effect of *rny* mutation on *ska* mRNA being counteracted by reduced *fasX* abundance, the net outcome of which is unchanged *ska* mRNA stability. A thorough screen of the *S. pyogenes* genome suggests that *fasX* is the only RNA that is destabilized by an RNase Y mutation (data not shown). The mechanism to explain this observation remains unclear and is worthy of further investigation.

RNase Y-mediated mRNA processing in the well-studied *gapA* operon of *B. subtilis* has been previously described (42). RNase Y mediates the mRNA cleavage between the *cggR* and *gapA* protein-coding regions, which leads to decreased stability of the *cggR*-containing transcript and increased stability of the *gapA*-containing transcript (10). We found in this and a previous study (25) that RNase Y was involved in the processing of two functionally related mRNAs, *speB* and *ropB*. Both mRNAs were processed in the 5′ untranslated region (UTR) and were stabilized after processing. These findings support the idea that RNA processing plays an important role in posttranscriptional regulation. The identification of processed RNAs on a genome-wide scale has been a challenge for traditional microarray analysis because RNA processing does not usually lead to an obvious change in mRNA abundance (35). However, since RNA processing changes the stability of mRNAs, those mRNAs that display segmental stability are very likely processed by some endoribonuclease(s). We are currently using this approach to search for processed RNAs in the *S. pyogenes* genome.

The finding that the *speB* and *ropB* mRNAs overlap is in agreement with a previous study by Neely et al. (38). Two possible regulatory mechanisms may underlie this unique chromosomal arrangement. Overlapping promoters can function as a repression-activation switch, where one promoter is turned on and the other is simultaneously turned off by the same regulatory protein (43). We have observed that the *speB* gene is highly expressed only in the late exponential and stationary phases, while the *ropB* gene is constitutively expressed in the exponential phase but rapidly diminished in expression after entry into the stationary phase (25). The distinct expression profiles of the two genes imply that such a regulatory mechanism might exist for the *speB-ropB* gene pair. Another possibility is that the 5′ UTR of the *ropB* mRNA, after RNase Y processing, may form a small antisense RNA that binds to the *speB* mRNA and modulates its stability. These two possibilities are under investigation in our laboratory.

RNase P is an essential endoribonuclease that catalyzes the maturation of tRNAs. Its catalytic function is achieved by an RNA component encoded by *rnpB* (40). We found in this study that RNase Y is responsible for the rapid degradation of *rnpB* read-through transcripts. A similar observation has been made in *E. coli*, where RNase E mediates the degradation of *rnpB* read-through transcripts (44). The RNase P RNA is extremely stable in the WT of both species, where all RNases are present. The presence of extra sequences upstream and/or downstream of the *rnpB* sequence makes the read-through transcript much more susceptible to RNase attack. It is unlikely that the extra nucleotides alter the secondary structure of the endogenous *rnpB* transcript, since Ko et al. have observed identical secondary structures in the *rnpB* mRNAs with and without extra nucleotides (44). It is possible that RNase E/Y cleaves the extended sequences with high efficiency and that the cleaved RNAs bearing monophosphates at the 5′ end are the preferred substrates for further degradation. Although the exact mechanism of the RNase Y action remains to be elucidated, our results clearly show that RNase Y is crucial for the rapid degradation of read-through transcripts containing highly structured sequences.

## ACKNOWLEDGMENTS

J.K. was supported by NIH/NIDCR grant R00DE018400.

We thank Justin Merritt (University of Oklahoma Health Sciences Center, Microbiology and Immunology) for helpful discussions.

## REFERENCES

1. **Andrade JM, Pobre V, Silva IJ, Domingues S, Arraiano CM.** 2009. The role of 3′-5′ exoribonucleases in RNA degradation. Prog. Mol. Biol. Transl. Sci. **85**:187–229.
2. **Mudd EA, Krisch HM, Higgins CF.** 1990. RNase E, an endoribonuclease, has a general role in the chemical decay of Escherichia coli mRNA: evidence that rne and ams are the same genetic locus. Mol. Microbiol. **4**:2127–2135.
3. **Condon C.** 2003. RNA processing and degradation in *Bacillus subtilis*. Microbiol. Mol. Biol. Rev. **67**:157–174.
4. **Lehnik-Habrink M, Lewis RJ, Mäder U, Stülke J.** 2012. RNA degradation in *Bacillus subtilis*: an interplay of essential endo- and exoribonucleases. Mol. Microbiol. **84**:1005–1017.
5. **Carpousis AJ, Luisi BF, McDowall KJ.** 2009. Endonucleolytic initiation of mRNA decay in Escherichia coli. Prog. Mol. Biol. Transl Sci. **85**:91–135.
6. **Shahbabian K, Jamalli A, Zig L, Putzer H.** 2009. RNase Y, a novel endoribonuclease, initiates riboswitch turnover in *Bacillus subtilis*. EMBO J. **28**:3523–3533.
7. **Lehnik-Habrink M, Newman J, Rothe FM, Solovyova AS, Rodrigues C, Herzberg C, Commichau FM, Lewis RJ, Stülke J.** 2011. RNase Y in *Bacillus subtilis*: a natively disordered protein that is the functional equivalent of RNase E from *Escherichia coli*. J. Bacteriol. **193**:5431–5441.
8. **Lehnik-Habrink M, Schaffer M, Mäder U, Diethmaier C, Herzberg C, Stülke J.** 2011. RNA processing in *Bacillus subtilis*: identification of targets of the essential RNase Y. Mol. Microbiol. **81**:1459–1473.
9. **Liou GG, Jane WN, Cohen SN, Lin NS, Lin-Chao S.** 2001. RNA degradosomes exist in vivo in *Escherichia coli* as multicomponent complexes associated with the cytoplasmic membrane via the N-terminal region of ribonuclease E. Proc. Natl. Acad. Sci. U. S. A. **98**:63–68.
10. **Commichau FM, Rothe FM, Herzberg C, Wagner E, Hellwig D, Lehnik-Habrink M, Hammer E, Völker U, Stülke J.** 2009. Novel activities of glycolytic enzymes in *Bacillus subtilis*: interactions with essential proteins involved in mRNA processing. Mol. Cell Proteomics **8**:1350–1360.
11. **Carpousis AJ.** 2007. The RNA degradosome of Escherichia coli: an mRNA-degrading machine assembled on RNase E. Annu. Rev. Microbiol. **61**:71–87.
12. **Mackie GA.** 1998. Ribonuclease E is a 5′-end-dependent endonuclease. Nature **395**:720–723.
13. **Durand S, Gilet L, Bessières P, Nicolas P, Condon C.** 2012. Three essential ribonucleases-RNase Y, J1, and III-control the abundance of a majority of *Bacillus subtilis* mRNAs. PLoS Genet. **8**:e1002520. doi:10.1371/journal.pgen.1002520.
14. **Marincola G, Schäfer T, Behler J, Bernhardt J, Ohlsen K, Goerke C, Wolz C.** 2012. RNase Y of *Staphylococcus aureus* and its role in the activation of virulence genes. Mol. Microbiol. **85**:817–832.
15. **Cunningham MW.** 2000. Pathogenesis of group A streptococcal infections. Clin. Microbiol. Rev. **13**:470–511.
16. **Kreth J, Chen Z, Ferretti J, Malke H.** 2011. Counteractive balancing of transcriptome expression involving CodY and CovRS in *Streptococcus pyogenes*. J. Bacteriol. **193**:4153–4165.
17. **Steiner K, Malke H.** 2002. Dual control of streptokinase and streptolysin S production by the covRS and fasCAX two-component regulators in Streptococcus dysgalactiae subsp. equisimilis. Infect. Immun. **70**:3627–3636.
18. **Treviño J, Perez N, Ramirez-Peña E, Liu Z, Shelburne SA, III, Musser JM, Sumby P.** 2009. CovS simultaneously activates and inhibits the CovR-mediated repression of distinct subsets of group A *Streptococcus* virulence factor-encoding genes. Infect. Immun. **77**:3141–3149.
19. **Carroll RK, Musser JM.** 2011. From transcription to activation: how group A streptococcus, the flesh-eating pathogen, regulates SpeB cysteine protease production. Mol. Microbiol. **81**:588–601.
20. **Le Rhun A, Charpentier E.** 2012. Small RNAs in streptococci. RNA Biol. **9**:414–426.
21. **Ramirez-Peña E, Treviño J, Liu Z, Perez N, Sumby P.** 2010. The group A *Streptococcus* small regulatory RNA FasX enhances streptokinase activity by increasing the stability of the ska mRNA transcript. Mol. Microbiol. **78**:1332–1347.
22. **Deltcheva E, Chylinski K, Sharma CM, Gonzales K, Chao Y, Pirzada ZA, Eckert MR, Vogel J, Charpentier E.** 2011. CRISPR RNA maturation by trans-encoded small RNA and host factor RNase III. Nature **471**:602–607.
23. **Barnett TC, Bugrysheva JV, Scott JR.** 2007. Role of mRNA stability in growth phase regulation of gene expression in the group A streptococcus. J. Bacteriol. **189**:1866–1873.
24. **Kang SO, Caparon MG, Cho KH.** 2010. Virulence gene regulation by CvfA, a putative RNase: the CvfA-enolase complex in Streptococcus pyogenes links nutritional stress, growth-phase control, and virulence gene expression. Infect. Immun. **78**:2754–2767.
25. **Chen Z, Itzek A, Malke H, Ferretti JJ, Kreth J.** 2012. Dynamics of speB mRNA transcripts in *Streptococcus pyogenes*. J. Bacteriol. **194**:1417–1426.
26. **McShan WM, Ferretti JJ, Karasawa T, Suvorov AN, Lin S, Qin B, Jia H, Kenton S, Najar F, Wu H, Scott J, Roe BA, Savic DJ.** 2008. Genome sequence of a nephritogenic and highly transformable M49 strain of *Streptococcus pyogenes*. J. Bacteriol. **190**:7773–7785.
27. **Lyon WR, Gibson CM, Caparon MG.** 1998. A role for trigger factor and an rgg-like regulator in the transcription, secretion and processing of the cysteine proteinase of Streptococcus pyogenes. EMBO J. **17**:6263–6275.
28. **Ajdić D, Pham VT.** 2007. Global transcriptional analysis of Streptococcus mutans sugar transporters using microarrays. J. Bacteriol. **189**:5049–5059.
29. **Abramoff MD, Magelhaes PJ, Ram SJ.** 2004. Image processing with ImageJ. Biophotonics Intl. **11**:36–42.
30. **Selinger DW, Saxena RM, Cheung KJ, Church GM, Rosenow C.** 2003. Global RNA half-life analysis in *Escherichia coli* reveals positional patterns of transcript degradation. Genome Res. **13**:216–223.
31. **Troutt AB, McHeyzer-Williams MG, Pulendran B, Nossal GJ.** 1992. Ligation-anchored PCR: a simple amplification technique with single-sided specificity. Proc. Natl. Acad. Sci. U. S. A. **89**:9823–9825.
32. **Steglich C, Lindell D, Futschik M, Rector T, Steen R, Chisholm SW.** 2010. Short RNA half-lives in the slow-growing marine cyanobacterium *Prochlorococcus*. Genome Biol. **11**:R54. doi:10.1186/gb-2010-11-5-r54.
33. **Tatusov RL, Koonin EV, Lipman DJ.** 1997. A genomic perspective on protein families. Science **278**:631–637.
34. **Bernstein JA, Khodursky AB, Lin PH, Lin-Chao S, Cohen SN.** 2002. Global analysis of mRNA decay and abundance in *Escherichia coli* at single-gene resolution using two-color fluorescent DNA microarrays. Proc. Natl. Acad. Sci. U. S. A. **99**:9697–9702.
35. **Kristoffersen SM, Haase C, Weil MR, Passalacqua KD, Niazi F, Hutchison SK, Desany B, Kolstø AB, Tourasse NJ, Read TD, Økstad OA.** 2012. Global mRNA decay analysis at single nucleotide resolution reveals segmental and positional degradation patterns in a Gram-positive bacterium. Genome Biol. **13**:R30. doi:10.1186/gb-2012-13-4-r30.
36. **Lee K, Bernstein JA, Cohen SN.** 2002. RNase G complementation of rne null mutation identifies functional interrelationships with RNase E in Escherichia coli. Mol. Microbiol. **43**:1445–1456.
37. **Chaussee MS, Ajdic D, Ferretti JJ.** 1999. The rgg gene of Streptococcus pyogenes NZ131 positively influences extracellular SPE B production. Infect. Immun. **67**:1715–1722.
38. **Neely MN, Lyon WR, Runft DL, Caparon M.** 2003. Role of RopB in growth phase expression of the SpeB cysteine protease of *Streptococcus pyogenes*. J. Bacteriol. **185**:5166–5174.
39. **Claessen D, Emmins R, Hamoen LW, Daniel RA, Errington J, Edwards DH.** 2008. Control of the cell elongation-division cycle by shuttling of PBP1 protein in *Bacillus subtilis*. Mol. Microbiol. **68**:1029–1046.
40. **Kazantsev AV, Pace NR.** 2006. Bacterial RNase P: a new view of an ancient enzyme. Nat. Rev. Microbiol. **4**:729–740.
41. **Hambraeus G, von Wachenfeldt C, Hederstedt L.** 2003. Genome-wide survey of mRNA half-lives in Bacillus subtilis identifies extremely stable mRNAs. Mol. Genet. Genomics **269**:706–714.
42. **Meinken C, Blencke HM, Ludwig H, Stülke J.** 2003. Expression of the glycolytic gapA operon in *Bacillus subtilis*: differential syntheses of proteins encoded by the operon. Microbiology **149**(Pt 3):751–761.
43. **Bendtsen KM, Erdossy J, Csiszovszki Z, Svenningsen SL, Sneppen K, Krishna S, Semsey S.** 2011. Direct and indirect effects in the regulation of overlapping promoters. Nucleic Acids Res. **39**:6879–6885.
44. **Ko JH, Han K, Kim Y, Sim S, Kim KS, Lee SJ, Cho B, Lee K, Lee Y.** 2008. Dual function of RNase E for control of M1 RNA biosynthesis in *Escherichia coli*. Biochemistry **47**:762–770.